

Array tracking of the volcanic tremor source at Deception Island, Antarctica

J. Almendros¹, J.M. Ibáñez^{1,2}, G. Alguacil^{1,2}, E. Del Pezzo³, and R. Ortiz⁴

Abstract. We have found experimental evidence which shows that the volcanic tremor recorded at Deception Island (South Shetland Islands, Antarctica) is a superposition in time of overlapping hybrid events. We studied data from a small aperture seismic array. Data analysis for tremor and hybrids included: (1) spectral analysis; (2) apparent slowness and back-azimuth determination by using the zero-lag cross-correlation method; and (3) polarization analysis. Both types of events share these common features: (a) two dominant spectral bands at frequencies 1-3 Hz (the most energetic) and 4-8 Hz; (b) several coherent phases with the same back-azimuth to the source and apparent slowness along the whole signal; (c) in the high frequency band, the apparent slowness is very low (around 0.17 s/km), indicating the propagation of body waves; (d) in the low frequency band, the apparent slowness is high (around 1.6 s/km), consistent with the presence of surface waves; and (e) clear P-wave onset followed by a complex pattern of Rayleigh waves. Therefore, both types of events are strongly related because they share the same source region, the same wave-propagation properties, and the same wave composition. Moreover, several arrivals, that resemble a single hybrid event, have been found along the tremor signals. Due to these reasons, we hypothesize that volcanic tremor of Deception Island is a superposition of hybrid type events. The source of both types could be the interaction between thaw water and hot materials in a shallow aquifer.

Introduction

Among the seismic signals generated by volcanoes, volcanic tremor is the most characteristic and complex. Several studies have been performed to understand the source mechanism and the composition of volcanic tremor. Many models have been proposed to explain the volcanic tremor sources related to different kinds of volcanic activity (Aki et al., 1977; Julian, 1994; McNutt, 1986; Schick, 1992; and Chouet, 1996). Spectral analysis shows that the volcanic tremor spectrum is mainly dominated by one or more peaks at frequencies below 3 Hz, independent of the type of volcanism. Many researchers have found that these peaks must be due to a source rather than a path or site effects (Fehler, 1983; Ferrazzini et al., 1991), considering them as governed by the dimension of the plumbing system. However, other authors (Goldstein and Chouet, 1994) suggested that path effects could be also responsible for some of the observed spectral features. Although the majority of the studies have shown that the tremor wavefield is composed of surface waves (McNutt, 1986; Gordeev

et al., 1990; Ferrazzini et al., 1991), body waves have also been shown to exist (Goldstein and Chouet, 1994). Polarization analyses (Seidl and Hellweg, 1991), waveform studies (Fehler, 1983), and other techniques (Chouet, 1996), have pointed out that volcanic tremor consists of many simple overlapping wavegroups radiated by time-discrete sources.

The present study was performed at Deception Island (62° 59' S, 60° 41' W), an active volcano located at the spreading centre of the Bransfield Strait back-arc on the southwestern side of the Scotia Sea region, Antarctica (Klepets and Lawver, 1996). A small aperture seismic array was deployed in an almost flat zone close to the Spanish Station. It was composed of 15 Mark L25B seismometers with extended response flat down to 1 Hz and 3 three-component Mark L4C seismometers with extended response between 0.1 and 48 Hz, in a triangle-shaped configuration about 500 m wide (Figure 1). Each channel operated with GPS time, with sampling frequency of 200 sps and with local digital recording on a PC (Alguacil et al., 1996). This array was in operation during two summer field surveys (one from December 1994 to March 1995 and another from December 1995 to March 1996) in order to monitor the seismic activity. Data records contain a wide variety of seismic signals, ranging from tectonic earthquakes of intermediate depth (Ibáñez et al., 1997) and local earthquakes (Vila et al., 1995) to long-period events, hybrid events (following the classification of Lahr et al., 1994) with a high-frequency first onset more pronounced than the first onset of the long-period events, and volcanic tremor. A detailed study of the whole seismic activity is reported in Ibáñez et al. (1996).

In this paper we study several episodes of volcanic tremor and hybrid events, that occurred in a three-days time interval. Three techniques were used: (1) spectral analysis in order to determine the spectral features; (2) ray parameter estimations by using array methods; and (3) polarization studies to investigate the nature of the wave field. We compare the results obtained for the volcanic tremor with those obtained for the hybrid events, and analyze the possible relationship between the sources of both types of events.

Data analysis

We have analyzed, among the 92 events recorded during the 3-days period (from January 19 to 21, 1996), 21 digital records of volcanic tremor and 20 hybrid events, selected on the basis of the best signal to noise ratio. A thermal-paper drum continuous monitor station which operated close to the array site ensures that these tremor episodes are the most energetic part of a continuous tremor lasting from minutes to some hours. The recorded tremors start abruptly enough to trigger the STA/LTA detection algorithm, sometimes with a clear onset, but due to the limited duration of the records (150 s), we have available only time limited samples of the whole tremor signal. Hybrid events have durations ranging from 40 to 70 seconds, with amplitudes in the seismogram similar to those for volcanic tremors. Array-averaged spectra and spectrograms of each event were obtained by FFT spectra of 1024-point moving windows shifted 512 points each step along the whole signal (Figure 2). They reveal that the maximum spectral peaks are in the range 1-3 Hz, and that a significant amount of energy is also present in the 4-8 Hz band. There is only one high-frequency peak in the

¹Instituto Andaluz de Geofísica, Universidad de Granada, Spain.

²Departamento de Física Teórica y del Cosmos, Universidad de Granada, Spain.

³Dipartimento di Fisica, Università di Salerno, Italy.

⁴Departamento de Vulcanología, Museo Nacional de Ciencias Naturales - CSIC, Madrid, Spain.

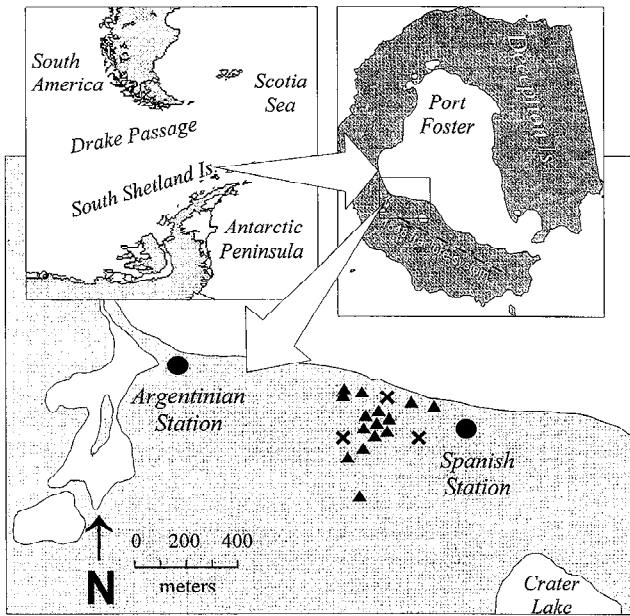


Figure 1. Map of Deception Island showing its location in the Scotia Sea region, the array site close to the Spanish Station and the array configuration, almost triangular, with a densely covered center. (★) Vertical Mark L25B stations. (×) Three-component Mark L4C stations.

spectrogram of hybrids, just at the beginning, while for tremor there are several sporadic high-frequency bursts along the signal. The low-frequency peaks follow in time the high-frequency ones, and are continuously present in the spectrograms of both kind of events. The peaks at low frequency shift from one tremor episode to another, as well as inside the same tremor event. Moreover, the spectra of tectonic local events (Ibáñez et al., 1997) do not show predominant peaks at the same frequency band. Therefore, we are confident that these low frequency peaks are more related to source processes than site or path effects.

On the basis of the results from spectral analysis, we filtered the seismograms in two bands (1-3 and 4-8 Hz) using a 5-pole Butterworth filter. Then, we applied the zero-lag cross-correlation method (Frankel et al., 1991) to the filtered seismograms in order to determine the apparent slowness across the array and the back-azimuth to the associated source. We used a moving window (80 points long for the high frequency band and 200 points long for the low frequency band) sliding in time one half window length each step, and beginning at the pre-event seismic noise. For each step and frequency band, the maximum averaged cross-correlation (hereafter, MACC) was calculated to obtain back-azimuth and apparent slowness for both type of events. Error limits are discussed in Del Pezzo et al. (1997), who show two main sources of error: one due to the array geometry, time sampling and grid search, and the other due to the seismic noise and the lack of coherence of the signal across the array. A joint evaluation of both provides us an uncertainty correlation level that is subtracted from MACC, leading to the determination of an error ellipse in the slowness plane. The average values of errors are 10° in back-azimuth and 0.02 s/km and 0.2 s/km respectively for high- and low-frequency in apparent slowness. For the pre-event seismic noise, the averaged MACC values are 0.15 (σ_l) for the low frequency band and 0.10 (σ_h) for the high frequency band. We selected solutions with MACC values greater than three times σ_l and five times σ_h , respectively. In Figure 3 we show histograms of all these selected solutions for both type of events and frequency bands.

Two distinct ranks of apparent slowness are observed for the two frequency bands. At low frequency, the calculated apparent slowness range between 1 and 2 s/km (apparent velocities between 0.5 and 1 km/s) with a dominant value of 1.6 s/km. At high frequency, we observe apparent slowness values down to 0.12 s/km (velocities up to 8 km/s) with a dominant value of 0.17 s/km.

Apparent slowness values at low frequency are compatible with the presence of surface waves in a low velocity medium (e.g. a volcanic environment), while the higher apparent velocity at high frequency indicates the presence of body waves. A similar result was also observed by Goldstein and Chouet (1994) in the shallow tremor of Kilauea volcano (Hawaii). Also two main directions for the back-azimuth to the source were obtained for the two frequency bands. We obtained most part of the solutions between 180° and 220° clockwise from north at low frequency, and between 120° and 140° , mainly around 130° , at high frequency. This difference in back-azimuth is an open question that have to be explained in further studies. It can be easily inferred from Figure 3 that both tremor and hybrid events share the same back-azimuth and apparent slowness distributions for both frequency bands. Figure 4 shows that MACC values are also dependent on the window position along the signal. At low frequency, solutions with high MACC are uniformly distributed along the signal. At high frequency, the pattern for hybrids is different from that for tremor. While these best correlated arrivals are located only at the beginning of the signal for the hybrid event, the good solutions appear suddenly several times along the signal for the volcanic tremor, coincident with the arrival of high-frequency wave packets and therefore with high-frequency bursts in the spectrogram of the signal.

Furthermore, low-MACC solutions for back-azimuth and apparent slowness in the high frequency band are sparse on a broad range covering 360° in azimuth and 0.12-0.75 s/km in apparent slowness (1-8 km/s in apparent velocity). This sparse distribution of low-MACC solutions is consistent with the presence of wave packets scattered by randomly distributed heterogeneity (Del Pezzo et al., 1997).

To study the wave composition of tremor, polarization analysis was performed using particle motion plots, checking the results with polarigrams and products of vertical, radial and transverse components (see e.g. Goldstein and Chouet, 1994) and polarization filters (Montalbetti and Kanasevich, 1970). The analysis reveals the

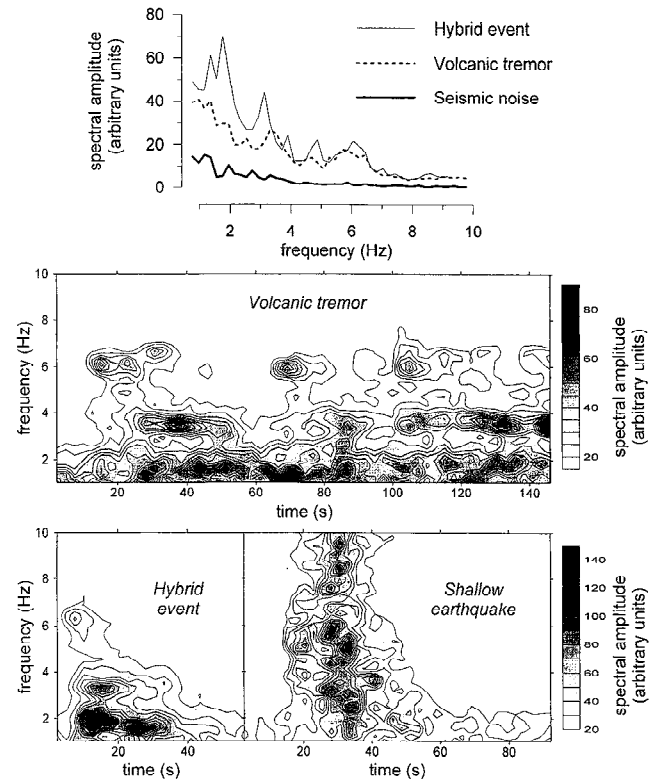


Figure 2. (top) Array-averaged spectra of volcanic events and seismic noise. (bottom) Array-averaged spectrograms of a volcanic tremor, a hybrid event, and a shallow local tectonic earthquake reported for a comparison. No peaks appear in the low-frequency band for tectonic events where hybrids and tremors are mainly peaked.

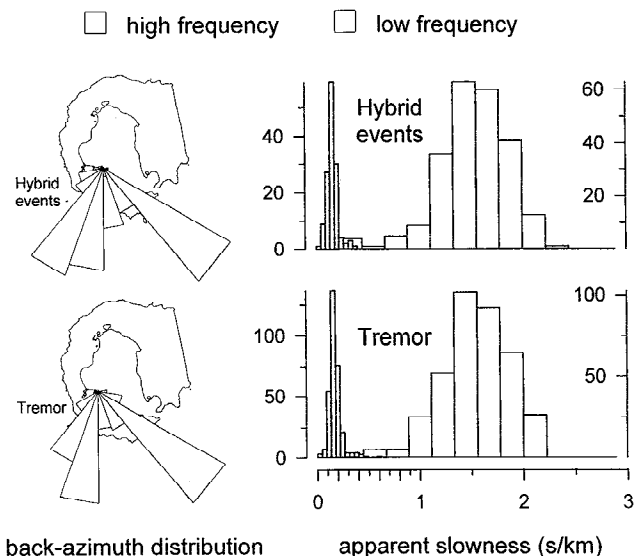


Figure 3. Bar plots of the high-MACC solutions for the analyzed hybrids (*top*) and tremor (*bottom*). *Left column:* distribution of back-azimuths from the array center. *Right column:* distribution of apparent slowness across the array site. The vertical axes of right graphs show the number of MACC solutions over $3\sigma_L$ for the low frequency band and $5\sigma_H$ for the high frequency band (see text for explanations).

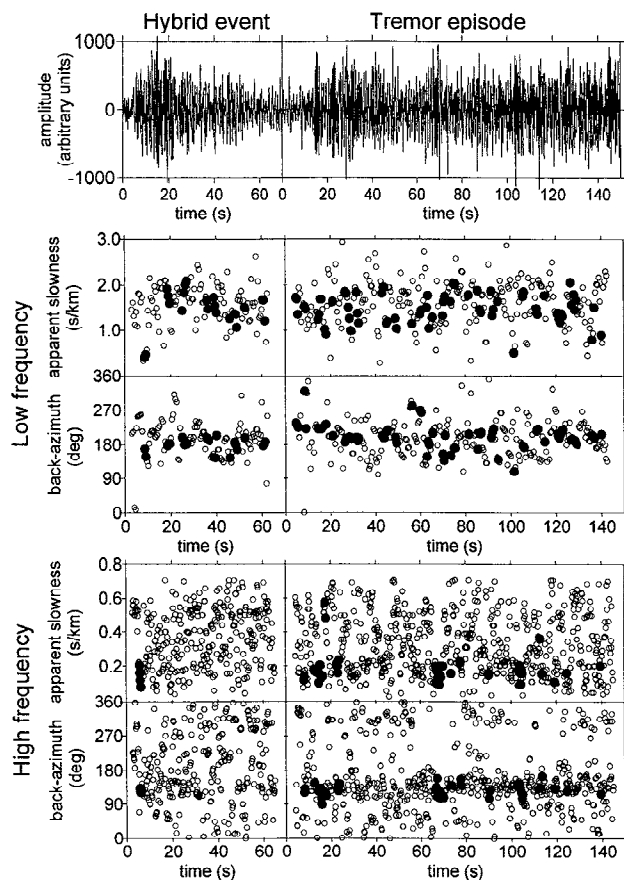


Figure 4. Whole unfiltered seismogram (*top*), and plots of apparent slowness and back-azimuth clockwise from North versus time in the 1-3 Hz frequency band (*center*) and in the 4-8 Hz frequency band (*bottom*) of a hybrid event (*left column*) and a volcanic tremor (*right column*). Time and amplitude scales are the same. Small circles are plotted for MACC below $3\sigma_L$ ($5\sigma_H$), and filled circles for MACC over $3\sigma_L$ ($5\sigma_H$), where σ_L (σ_H) is the averaged MACC for the pre-event noise at the low (high) frequency band.

presence of a complex pattern of surface waves at low frequency, mainly composed of Rayleigh waves. At high frequency the correlated arrivals are composed by highly linear, almost radially polarized wave packets with durations from 0.5 to 2.5 seconds, possibly P-waves. Clear shear wave phases were not observed inside the best correlated intervals. The above results are valid for both tremor and hybrid events. In Figure 5 we show an example of the high frequency particle motion pattern for a volcanic tremor sample and for a hybrid event. For both we show the first onset, because this is the only portion of the seismogram in which the waves are less perturbed by other wave arrivals. It can be observed from the plots that the ground motion is strongly polarized along the radial component, with little contribution of SV and SH component. This result indicates the possible presence of a P-wave in both cases.

Conclusions and Discussion

The array analysis of volcanic tremors at Deception Island shows the presence of well correlated wave packets composed of surface and body waves coming from the same back-azimuth. The polarization analysis reveals that the body waves are mostly P-

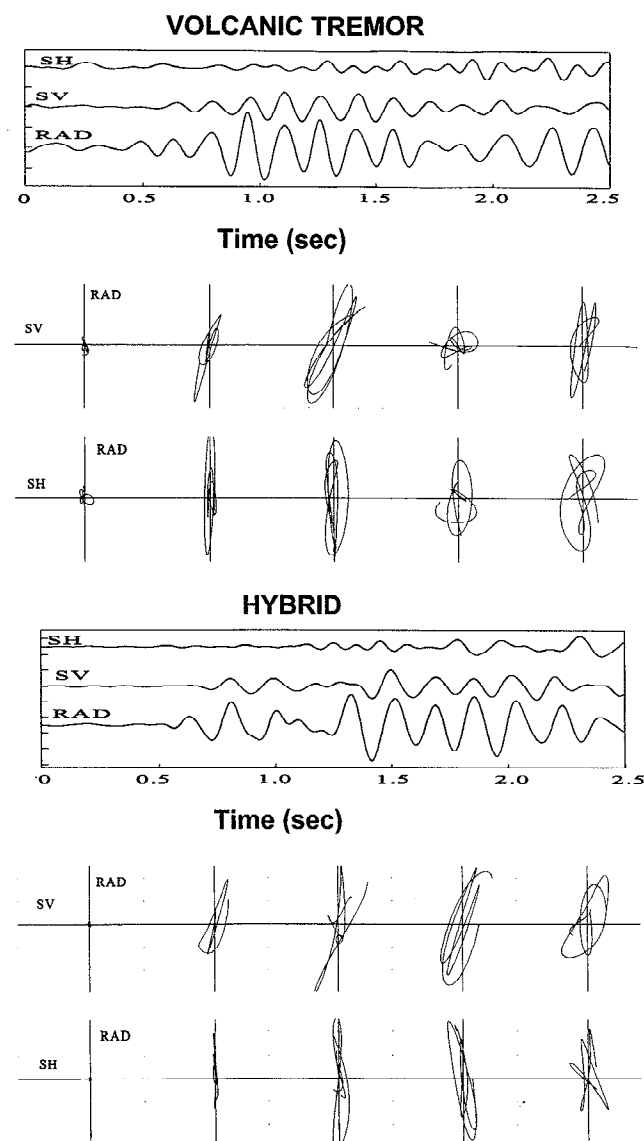


Figure 5. Comparison of the particle motion of tremors with that for hybrids. We show the first 2 seconds of the high-frequency, filtered, rotated, three-component seismograms, and the corresponding particle motion plots.

waves, and that surface waves are mainly Rayleigh waves. The comparison between hybrids and tremor suggests that both kind of events share the same source region and mechanism, and we conclude that tremor is composed by hybrid-type events which occur in temporally dense swarms. This conclusion rests on: (a) the spectral similarity of volcanic tremor and hybrids; (b) the similar polarization pattern; (c) the same back-azimuth distribution at low and high frequency; (d) the same apparent slowness values for both frequency bands; (e) the existence of several high-frequency bursts in the tremor spectrogram that resemble the spectrogram of a single hybrid event; and (f) volcanic tremors show well-correlated high-frequency wave packets along the seismogram with the same back-azimuth and apparent slowness found for hybrids.

Although the real position of the source is not determined in depth and distance, the stability of the solutions reveals that the source location is the same during the analyzed swarm. Every spatial change in the position of the source would in fact be reflected by a change in the back-azimuth and apparent slowness. Therefore, hybrids and volcanic tremor share the same source region. At the present, there is not an active vent on Deception Island, and therefore we cannot directly relate the source with transport of magma and other fluids in an active channel.

The existence of recent eruptions (e.g. 1842, 1912, 1917, 1967, 1969, 1970), the special weather conditions, the presence of many glacials that in summer provide a huge quantity of thaw water, and the existence of shallow and confined water-saturated layers (Martí and Baraldo, 1990) make us to suppose that the most likely source mechanism involves the interaction between water and hot materials. It should be pointed out that the high-frequency observed in tremor seismograms may be detected only close to the source because of the high seismic attenuation of most volcanic areas (Q as low as 11, see e.g. Vila et al., 1995). Therefore, the source must be located very close to the array site. The average back-azimuth direction for high frequency solutions of the swarm source is toward the Crater Lake (see Figure 1). This back-azimuth line crosses a very recent fracture system about 2 km southward the Crater Lake, where a strombolian eruption took place in 1842 (González-Ferrán, 1995). We suppose that this fracture system is the most likely source region of the swarm. The possible presence of high temperature materials in the vicinity of this fracture system could lead to abrupt water-steam phase changes producing a step pressure that generates a hybrid event. The tremor episodes would occur when the phenomenon of water-steam phase change reaches a critical stage.

Acknowledgements. This paper has been partially supported by the projects *ANT94-0854-C02* and *ANT95-0994-C03*, by *Grupo de Investigación en Geofísica J.A.4057* and by *Italy's GNV (Grupo Nazionale di Vulcanologia CNR)*. We gratefully acknowledge Dr. José Morales and three anonymous reviewers for their useful comments; Spanish Army and Navy for providing us with logistic help during the antarctic surveys in the Gabriel de Castilla Station; and all the participants in the two surveys at Deception Island, specially to Mr. Rafael Abella and Dr. Manuel Berrocoso, for their help and cooperation.

References

- Aki, K., M.Fehler, S.Das. Source mechanism of volcanic tremor: Fluid-driven crack models and their application to the 1963 Kilauea eruption, *Journ. Volcan. Geotherm. Res.*, **2**, 259-287, 1977.
- Alguacil, G., R.Ortiz, J.C.Olmedillas, E.Del Pezzo, J.M.Ibáñez, Desarrollo de arrays sísmicos para la monitorización de la actividad tectónica y volcánica en la Antártida, *VI Spanish Symposium on Antarctic Studies*, Madrid, 1996.
- Chouet, B., Long-period volcano seismicity: its source and use in eruption forecasting, *Nature*, **380**, 309-316, 1996.
- Del Pezzo, E., M.Larocca, J.M.Ibáñez, Observations of high-frequency scattered waves using dense arrays, *Bull. Seism. Soc. Am.*, in press, 1997.
- Fehler, M., Observations of volcanic tremor at Mount St.Helens volcano, *Journ. Geophys. Res.*, **88**, 3476-3484, 1983.
- Ferrazzini, V., K.Aki and B.Chouet, Characteristics of seismic waves composing hawaiian volcanic tremor and gas-piston events observed by a near-source array, *Journ. Geophys. Res.*, **96**, 6199-6209, 1991.
- Frankel, A., S.Hough, P.Friberg and R.Busby, Observations of Loma Prieta aftershocks from a dense array in Sunmyvalc, California, *Bull. Seism. Soc. Am.*, **81**, 1900-1922, 1991.
- Goldstein, P. and B.Chouet, Array measurements and modelling of sources of shallow volcanic tremor at Kilauea volcano, Hawaii, *Journ. Geophys. Res.*, **99**, 2637-2652, 1994.
- González-Ferrán, O., *Volcanes de Chile*, 640 pp., Instituto Geográfico Militar, Santiago de Chile, 1995.
- Gordeev, E.L., V.A.Saltykov, V.I.Sinitin and V.N.Chebrov, Temporal and spatial characteristics of volcanic tremor wave fields, *Journ. Volcan. Geotherm. Res.*, **40**, 89-101, 1990.
- Ibáñez, J.M., E.Del Pezzo, R.Ortiz, J.Morales, G.Alguacil, J.Almendros, A.García, F.Vidal, Dos años de monitorización de la actividad sísmica de la Isla Decepción usando arrays sísmicos, *VI Spanish Symposium on Antarctic Studies*, Madrid, 1996.
- Ibáñez, J.M., J.Morales, G.Alguacil, J.Almendros, R.Ortiz, E.Del Pezzo, Intermediate-focus earthquakes under South Shetland Islands, Antarctica, *Geophys. Res. Lett.*, **24**, 531-534, 1997.
- Julian, B.R., Volcanic tremor: nonlinear excitation by fluid flow, *Journ. Geophys. Res.*, **99**, 11859-11877, 1994.
- Kepleis, K.A., L.A.Lawver, Tectonics of the Antarctic-Scotia plate boundary near Elephant and Clarence Islands, West Antarctica, *Journ. Geophys. Res.*, **101**, 20211-20231, 1996.
- Lahr, J.C., B.A.Chouet, C.D.Stephens, J.A.Power, R.A.Page, Earthquake classification, location, and error analysis in a volcanic environment: implications for the magmatic system of the 1989-1990 eruptions at Redoubt volcano, Alaska, *Journ. Volcan. Geotherm. Res.*, **62**, 137-151, 1994.
- Martí, J., A.Baraldo, Pre-caldera pyroclastic deposits of Deception Island (South Shetland Islands), *Antarctic Science*, **2**, 345-352, 1990.
- McNutt, S.R., Observations and analysis of B-type earthquakes, explosions and volcanic tremor at Pavlov volcano, Alaska, *Bull. Seism. Soc. Am.*, **76**, 153-175, 1986.
- Montalbetti, J.F., E.R.Kanasevich, Enhancement of teleseismic body phases with a polarization filter, *Geophys. J. R. Astr. Soc.*, **21**, 119-129, 1970.
- Schick, R., Volcanic tremor: seismic signals of (almost) unknown origin, in *Volcanic Seismology (IAVCEI Proceedings in Volcanology 3)*, P.Gasparini, R.Scarpa, K.Aki, 157-167, Springer-Verlag, Berlin, 1992.
- Scidl, D., M.Hellweg, Volcanic tremor recordings: polarization analysis, in *Volcanic tremor and magma flow (Scientific Series of the International Bureau 4)*, R.Schick, R.Mugiono, 31-47, Forschungszentrum Jülich GmbH (KFA), 1991.
- Vila, J., A. M. Correig, J. Martí, Attenuation and source parameters at Deception Island (South Shetland Islands, Antarctica), *Pur. Appl. Geophys.*, **144**, 229-250, 1995.

J.Almendros, J.M.Ibáñez and G.Alguacil. Instituto Andaluz de Geofísica, Universidad de Granada. Campus de Cartuja, s/n. 18071 Granada, Spain. (vikingo@platon.ugr.es, ibancz@gea.ugr.es, alguacil@gea.ugr.es,)
E.Del Pezzo. Dipartimento di Fisica, Università di Salerno, 84081 Baronissi, Salerno, Italy. (delpezzo@axpgeo.csied.unisa.it).
R.Ortiz. Museo Nacional de Ciencias Naturales - CSIC, Departamento de Vulcanología, José Gutiérrez Abascal 2, 28006 Madrid, Spain. (mncor72@pinar1.csic.es).

(Received: December 12, 1996; revised: June 20, 1997; accepted: October 3, 1997)